



ORIGINAL RESEARCH ARTICLE

OPEN ACCESS

## CHARACTERIZATION OF CASEIN PHOSHOPEPTIDE-AMORPHOUS CALCIUM PHOSPHATE BASED PRODUCTS WITH AND WITHOUT SODIUM FLUORIDE

<sup>1</sup>Xiaojing Chen, <sup>1</sup>Faiza Gulfam, <sup>\*2</sup>David G. Gillam and <sup>1</sup>Robert G. Hill

<sup>1</sup>Dental Physical Sciences, Institute of Dentistry, Queen Mary University of London, Mile End Road, London E1 4NS, United Kingdom

<sup>2</sup>Centre for Adult Oral Health, Barts and The London School of Medicine and Dentistry, Queen Mary University of London (QMUL), London E1 2AD, UK

### ARTICLE INFO

#### Article History:

Received 27<sup>th</sup> August 2017

Received in revised form

26<sup>th</sup> September, 2017

Accepted 11<sup>th</sup> October, 2017

Published online 30<sup>th</sup> November, 2017

#### Key Words:

Casein phosphopeptide-amorphous calcium phosphate, Fluoride, Remineralization, <sup>31</sup>P and <sup>19</sup>F MAS-NMR.

### ABSTRACT

**Aim:** The aim of this paper was to characterize the active ingredients of ACP remineralizing pastes MI Paste<sup>TM</sup> and MI Paste Plus<sup>TM</sup>.

**Materials and Method:** Two CPP-ACP containing products MI Paste<sup>TM</sup> and MI Paste Plus<sup>TM</sup> with addition of 900ppm sodium fluoride (NaF) supplied by GC America Inc. were evaluated. The free fluoride content of MI Paste Plus<sup>TM</sup> was quantified using a fluoride ion selective electrode (Orion 9609BN, 710A meter, South Burlington, VT, USA). 1.50 g of MI Paste Plus<sup>TM</sup> was dissolved thoroughly in 100 ml de-ionized water. Samples were prepared in duplicate. Ten grams of each product was weighed and mixed with 40ml of deionized water in a centrifuge tube. The solutions were vacuum filtered using a suction filtration setup, which consisted of a filter paper with pore size of 5-13 μm (Fisher Scientific, Loughborough), a Buchner funnel (250 ml, VWR, Leicestershire), a 500ml suction flask (Duran, Mainz) and a vacuum pump (KNF, Neuberger). The extracts were oven dried at 37°C for 24 hours prior to the further characterization by a combination usage of X-ray Diffraction (XRD), Fourier Transform Infrared Spectroscopy (FTIR) and <sup>31</sup>P and <sup>19</sup>F Magic Angle Spinning-Nuclear Magnetic Resonance (MAS-NMR).

**Results and Conclusions:** The characterization of the extracts from MI Paste<sup>TM</sup> and MI Paste Plus<sup>TM</sup> clearly demonstrated varying degrees of the conversion of the ACP to apatite. A more significant conversion was observed in the MI Paste Plus<sup>TM</sup> with soluble fluoride. The fluoride ions bound to calcium and phosphate ions to form chemically stable fluorapatite, which resulted in a deficiency of mineral ions for remineralization, subsequently reduced the remineralization rate. The usage of sodium monofluorophosphate as an alternative to sodium fluoride could, however prevent this undesired conversion.

#### \*Corresponding author

Copyright ©2017, Xiaojing Chena et al. This is an open access article distributed under the Creative Commons Attribution License, which permits unrestricted use, distribution, and reproduction in any medium, provided the original work is properly cited.

Citation: Xiaojing Chen, Faiza Gulfam, David G. Gillam and Robert G. Hill, 2017. "Characterization of casein phosphopeptide-amorphous calcium phosphate based products with and without sodium fluoride", *International Journal of Development Research*, 7, (11), 17221-17224.

### INTRODUCTION

Demineralization is a dissolution process of carbonated hydroxyapatite (HCP) minerals of hard tissues, such as enamel and dentine, releasing calcium and phosphate ions (Abou Neel et al., 2016). This demineralization process could be halved or reversed via the re-deposition of carbonated hydroxyapatite mineral (remineralization) by restoring adequate calcium, phosphate and fluoride ions prior to the initiation of dental

caries (Featherstone, 2000; Featherstone, 2008; ten, Cate, 1999). Fluoride therapy and the utilization of dental products containing calcium and phosphate are widely used as potentially curative regimes for tooth demineralization (Abou Neel et al., 2016; Reynolds, 2008). Fluoride is recognized to inhibit enamel demineralization (ten Cate, 1999; Lynch et al., 2004; Gorton and Featherstone, 2003) and assist in enamel remineralization and fluorapatite (FAP) formation (Ten, Cate, 1999). FAP is much more stable in an acidic environment than

hydroxyapatite, due to the fact that the fluoride ion is smaller than the hydroxyl ion (Moreno *et al.*, 1974) and fits into the plane of the Ca(II) triangle of the apatite lattice. Therefore, fluoride is particularly attractive and widely used in dental applications. Casein phosphopeptide (CPP) is also recognized for its ability to stabilize calcium and phosphate ions through the formation of soluble complexes, therefore, they not only prevent the precipitation of calcium phosphate but also provide a source of calcium and phosphate (Srinivasan *et al.*, 2010). It has been clinically proven that casein phosphopeptide-amorphous calcium phosphate (CPP-ACP) nanocomplexes, serving as a calcium and phosphate reservoir, are anticariogenic and facilitate the remineralization of the early stages of enamel caries in both animal and human studies (Cross *et al.*, 2016; Reynolds *et al.*, 1995; Reynolds *et al.*, 1999; Reynolds *et al.*, 2003).

A combination of CPP-ACP and fluoride was reported to show a superior remineralization effect over the individual use of either CPP-ACP or fluoride by Reynolds *et al.* (Srinivasan *et al.*, 2010; Reynolds *et al.*, 2008). However, our recent unpublished study of the remineralization rate of MI Paste™ (containing CPP-ACP) and MI Paste Plus™ (containing CPP-ACP plus 900 ppm sodium fluoride) demonstrated that the MI Paste™ remineralized enamel at a higher rate than MI Paste Plus™ with fluoride. This was unexpected as it was suggested that the addition of fluoride to MI Paste™ would result in a faster remineralization rate as fluoride promotes enamel remineralization. This observation also contradicted the finding by Reynolds *et al.* (2008). The aim of this study was to characterize the active ingredients of MI Paste™ and MI Paste Plus™ and provide a better understanding of the unexpected lower remineralization rate of MI Paste Plus™ containing both CPP-ACP and fluoride.

## MATERIALS AND METHODS

### Materials

Two CPP-ACP containing products MI Paste™ and MI Paste Plus™ with the addition of 900ppm sodium fluoride (NaF) supplied by GC America Inc. were evaluated.

### Fluoride ion release

The free fluoride content of MI Paste Plus™ was quantified using a fluoride ion selective electrode (Orion 9609BN, 710A meter, South Burlington, VT, USA). 1.50 g of MI Paste Plus™ was dissolved thoroughly in 100 ml de-ionized water. Samples were prepared in duplicate.

### The active ingredients extraction

Ten grams of each product was weighed and mixed with 40ml of deionized water in a centrifuge tube. The solutions were vacuum filtered using a suction filtration setup, which consisted of a filter paper with pore size of 5-13 μm (Fisher Scientific, Loughborough), a Buchner funnel (250 ml, VWR, Leicestershire), a 500ml suction flask (Duran, Mainz) and a vacuum pump (KNF, Neuberger). The extracts were oven dried at 37°C for 24 hours prior to the further characterization by a combination usage of X-ray Diffraction (XRD), Fourier Transform Infrared Spectroscopy (FTIR) and <sup>31</sup>P and <sup>19</sup>F Magic Angle Spinning-Nuclear Magnetic Resonance (MAS-NMR).

## Characterization of the extracts

### XRD

An X'Pert Pro X-ray diffractometer (PANalytical, Eindhoven, The Netherlands) was conducted with a Cu-Kα X-ray source. The XRD patterns were collected at a typical step size of 0.0334° between a 2θ range of 10 to 60 degrees.

### FTIR

A Fourier Transform Infrared Spectroscopy (Spectrum GX, Perkin-Elmer, Cambridge, UK) was also used to assess the obtained extracts. The data were recorded between 1600 to 500 cm<sup>-1</sup> in an absorbance mode.

### <sup>31</sup>P and <sup>19</sup>F MAS-NMR

<sup>31</sup>P and <sup>19</sup>F MAS-NMR experiments were undertaken at a spinning rate of 22 kHz in a 2.5 mm rotor on a 600 MHz (14.1T) Bruker NMR spectrometer (Bruker AV 600 NMR, Coventry, UK). <sup>31</sup>P and <sup>19</sup>F MAS-NMR were performed at Larmor frequencies of 242.9 MHz and 564.7 MHz, respectively. A recycle delay of 60s was applied for all the experiments and the spectra were collected after 32 scans. The chemical shifts of <sup>31</sup>P and <sup>19</sup>F were referenced against 85% H<sub>3</sub>PO<sub>4</sub> (δ 0.0 ppm) and 1M NaF (δ 120.0 ppm), respectively.

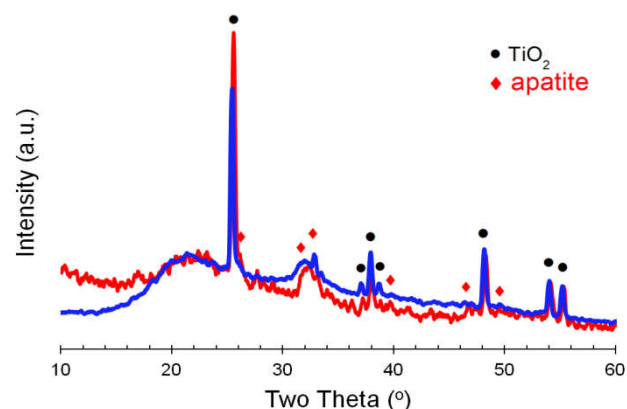


Figure 1. XRD Patterns of MI Paste™ (blue) and MI Paste Plus™ (red)

## RESULTS AND DISCUSSION

Sodium fluoride is a common additive in toothpastes. It is soluble in water, providing free fluoride ions for caries prevention. Surprisingly, the fluoride measurement shows an only 1.8 ppm free fluoride in the solution, rather than 13.5 ppm calculated based on the 900ppm specified by the manufacturer. This would suggest that most fluoride ions have probably been bound to another ingredient from within the MI Paste plus™ and the most likely component was the ACP. The XRD patterns of the solids extracted from MI Paste™ and MI Paste Plus™ were determined and are shown in Figure 1. The presence of rutile (TiO<sub>2</sub>) added as a whitening agent was revealed by observing sharp diffraction lines at values of approximately 25.7, 37.93, 48.2, 54.08 and 55.25° 2θ. More interestingly, two broad peaks were observed in the patterns, one at about 15-25° 2θ and the other at about 30-35° 2θ. The first broad peak at 15-25° 2θ corresponds to amorphous silica, which is typically added as a thickening agent to toothpaste

formulations, whereas the latter broad peak at  $30\text{-}35^\circ 2\theta$  may suggest the presence of the ACP (Cross *et al.*, 2004). Furthermore, minor peaks at  $26^\circ$ ,  $46.7^\circ$  and  $49.5^\circ$  matched to apatite diffraction lines were also observed in both XRD patterns.

The FTIR spectra of hydroxyapatite, MI Paste™ and MI Paste Plus™ are shown in Figure 2. Hydroxyapatite exhibits P-O vibrational modes at  $564\text{cm}^{-1}$  ( $\nu_4'$ ),  $600\text{cm}^{-1}$  ( $\nu_4''$ ) and  $1023\text{cm}^{-1}$  ( $\nu_3$ ). The FTIR spectrum of MI Paste Plus™ was very similar to that of MI Paste™, which contains all those vibrational bands though the  $\nu_4$  bands are relatively weaker and the  $\nu_3$  band was much broader compared to the equivalent features for HAP. The broad features are probably overlapped by the contributions from both the silica and casein phosphopeptide components. Furthermore, there was a small amount of carbonate in MI Paste™ and MI Paste Plus™ as indicated by bands at  $870\text{cm}^{-1}$  and in the range of  $1420\text{-}1470\text{cm}^{-1}$  (Chen *et al.*, 2014).

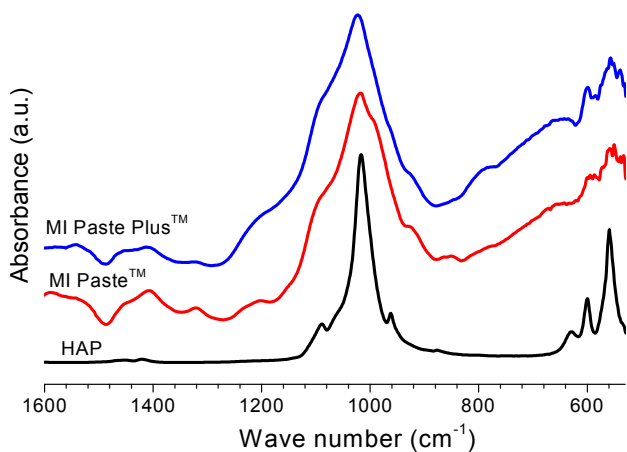


Figure 2. FTIR Spectrum of Hydroxyapatite, MI Paste™ and MI Paste Plus™

Figure 3 compares the  $^{31}\text{P}$  MAS-NMR spectra of MI Paste™ and MI Paste Plus™ to those of hydroxyapatite and an amorphous  $\text{SiO-CaO-P}_2\text{O}_5\text{-CaF}_2$  bioactive glass, GPF4.5 (Chen *et al.*, 2014). Glass GPF shows an amorphous calcium orthophosphate environment with a broad peak at around 3 ppm. Both spectra for MI Paste™ and MI Paste Plus™ exhibit a broad peak centred at about 2.8-2.9 ppm, while the peak for MI Paste™ was slightly broader, indicating a less ordered calcium orthophosphate environment in MI Paste™. A slight shoulder at around 2.0 ppm assigned to an acidic phosphate species, corresponding to P-OH groups was observed in the spectrum for MI Paste™. The chemical shifts observed were close to those for crystalline hydroxyapatite and fluorapatite, while the full width half maximums are located in between the glass GPF4.5 and the crystalline hydroxyapatite. These indicate the presence of a relatively well ordered calcium orthophosphate (apatite-like phase) environment. This apparently seems contradictory with the XRD data, indicating a largely amorphous nature for the active ACP ingredient in MI Paste™ and MI Paste Plus™. However it is important to note that X-ray diffraction probes long range order  $>5$  nm corresponding to more than 50 atomic spacings. Thus small nano crystals appear amorphous by XRD. MAS-NMR in contrast probes the local environment around a nucleus and investigates much shorter length scales.

In the  $^{31}\text{P}$  NMR spectra of MI Paste™ and MI Paste Plus™, it was also expected to observe signals from phosphorylated serine residues in the casein phosphopeptide at 0.6 and 4.9 ppm (Hoffmann *et al.*, 1994). Hoffmann *et al.* (1994) expected these signals to be of low intensity relative to the ACP. Here, these signals may be overlapping with crystalline calcium orthophosphate peaks and lead to the asymmetry at around 2.8-2.9 ppm.

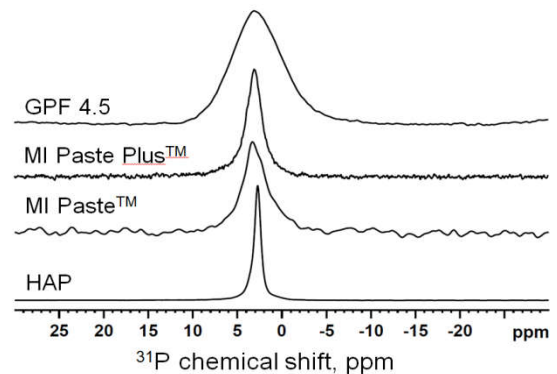


Figure 3.  $^{31}\text{P}$  MAS-NMR Spectra of Hydroxyapatite, MI Paste™, MI Paste Plus™ and bioactive glass GPF 4.5, adapted from (Chen *et al.*, 2014)

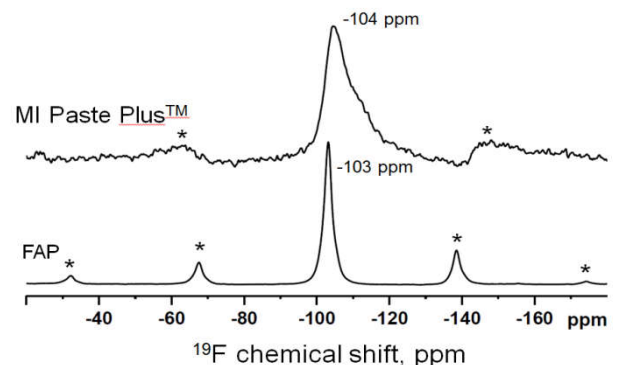


Figure 4.  $^{19}\text{F}$  MAS-NMR spectra of MI Paste Plus™ and FAP

The  $^{19}\text{F}$  spectrum for MI Paste Plus™ is shown in Figure 4 and compared with a typical spectrum for fluorapatite. No  $^{19}\text{F}$  NMR signal was obtained for the MI Paste™. In contrast, a strong signal was detected for the MI Paste Plus™ indicating that the fluoride was largely in the solid phase and no longer in the water soluble portion of the paste. The  $^{19}\text{F}$  MAS-NMR spectrum for MI Paste Plus™ exhibited a relatively broad feature with a chemical shift of -104 ppm close to that for the F-Ca(3) site of fluorapatite at -102 ppm. This broader peak with a slightly more negative chemical shift compared to that of typical fluorapatite indicated the formation of fluorapatite-like phase with a low degree of crystallinity and this fluorapatite-like phase may probably contain a relatively low OH content since the  $^{19}\text{F}$  chemical shift reduces slightly for mixed hydroxyl-fluorapatites (Gao *et al.*, 2016). Additionally, the spectrum for MI Paste Plus™ was asymmetric and had a shoulder at -108 ppm that probably corresponds to a F-Ca(4) like environment, similar to fluorite ( $\text{CaF}_2$ ) (Chen *et al.*, 2014). The presence of such a strong  $^{19}\text{F}$  signal from the solid phase explains the extremely low value for the measured fluoride content of MI Paste Plus™, since the free fluoride has reacted with the ACP phase and converted to fluorapatite-like phase. This reaction may take place immediately after manufacture or

occur during storage. The formation of a fluorapatite-like phase was likely to result in a more stable phase that will not provide free  $\text{Ca}^{2+}$  and  $\text{PO}_4^{3-}$  ions so readily for remineralization. This may explain the surprising lower remineralization rate of MI Paste Plus™ compared to MI paste™. A similar situation occurred when NaF was used in conjunction with nano hydroxyapatites where the fluoride was taken up by the hydroxyapatite and convert to a more stable fluorapatite (Hill *et al.*, 2015). This problem can largely be overcome by using sodium monofluorophosphate instead of NaF. In sodium monofluorophosphate the fluorine is covalent bound to phosphorus and is largely not released as the free fluoride ion until hydrolysis occurs by the enzyme alkaline phosphatase in saliva. The use of sodium monofluorophosphate, rather than NaF in MIPaste Plus™ could prevent the consumption of fluoride to form the fluorapatite-like species that may occur in the tube during storage.

## Conclusion

The characterization of the extracts from MI Paste™ and MI Paste Plus™ clearly demonstrated varying degrees of the conversion of the ACP to apatite. A more significant conversion was observed in the MI Paste Plus™ with soluble fluoride. The fluoride ions bound to calcium and phosphate ions to form chemically stable fluorapatite, which resulted in a deficiency of mineral ions for remineralization, subsequently reduced the remineralization rate. The usage of sodium monofluorophosphate as an alternative to sodium fluoride could, however prevent this undesired conversion.

## REFERENCES

- Abou Neel, E.A., Aljabo, A., Strange, A., Ibrahim, S., Coathup, M., Young, A.M., *et al.* 2016. Demineralization–remineralization dynamics in teeth and bone, *International Journal of Nanomedicine*, 11, 4743-63
- Chen, X., Chen, X., Brauer, D.S., Wilson, R.M., Hill, R.G., Karpukhina, N. 2014. Bioactivity of sodium free fluoride containing glasses and glass-ceramics, *Materials*, 7, 5470-87
- Chen, X., Chen, X., Brauer, D.S., Wilson, R.M., Hill, R.G., Karpukhina, N. 2014. Novel alkali free bioactive fluorapatite glass ceramics, *Journal of Non-Crystalline Solids*, 402, 172-7
- Cross K., Huq N., Stanton D., Sum M., Reynolds E. 2004. NMR studies of a novel calcium, phosphate and fluoride delivery vehicle- $\alpha$  S1-casein (59–79) by stabilized amorphous calcium fluoride phosphate nanocomplexes, *Biomaterials*, 25, 5061-9
- Cross, K.J., Huq, N.L., Reynolds, E.C. 2016. Casein Phosphopeptide–Amorphous Calcium Phosphate Nanocomplexes: A Structural Model, *Biochemistry*, 55, 4316-25
- Featherstone, J.D.B. 2000. The science and practice of caries prevention, *The Journal of the American Dental Association*, 131, 887-99.
- Featherstone, J.D.B. 2008. Dental caries: a dynamic disease process, *Australian Dental Journal*, 53, 286-91
- Gao, Y., Karpukhina N., Law R.V. 2016. Phase segregation in hydroxyfluorapatite solid solution at high temperatures studied by combined XRD/solid state NMR, *RSC Advances*, 6, 103782-90
- Gorton, J. and Featherstone, J.D.B. 2003. In vivo inhibition of demineralization around orthodontic brackets, *American Journal of Orthodontics and Dentofacial Orthopedics*, 123, 10-4
- Hill, R.G., Gillam, D.G., Chen X. 2015. The ability of a nano hydroxyapatite toothpaste and oral rinse containing fluoride to protect enamel during an acid challenge using 19F solid state NMR spectroscopy, *Materials Letters*, 156, 69-71
- Hoffmann, R., Reichert, I., Wachs, W.O., Zeppezauer, M., Kalbitzer, H.R. 1994. 1H and 31P NMR spectroscopy of phosphorylated model peptides, *International Journal of peptide and Protein Research*, 44, 193-8
- Lynch, R., Navada, R., Walia, R. 2004. Low-levels of fluoride in plaque and saliva and their effects on the demineralisation and remineralisation of enamel; role of fluoride toothpastes, *International Dental Journal*, 54, 304-9
- Moreno, E.C., Kresak, M., Zahradni, Rt. 1974. Fluoridated hydroxyapatite solubility and caries formation, *Nature*, 247, 64-5
- Reynolds, E. 2008. Calcium phosphate-based remineralization systems: scientific evidence?, *Australian Dental Journal*, 53, 268-73
- Reynolds, E., Black, C., Cai, F., Cross, K., Eakins, D., Huq, N., *et al.* 1999. Advances in enamel remineralization: casein phosphopeptide-amorphous calcium phosphate, *Journal of Clinical Dentistry*, 10, 86-8
- Reynolds, E., Cain, C., Webber, E., Black, C., Riley, P., Johnson, I., *et al.* 1995. Anticariogenicity of calcium phosphate complexes of tryptic casein phosphopeptides in the rat, *Journal of Dental Research*, 74, 1272-9
- Reynolds, E.C., Cai, F., Cochrane, N.J., Shen, P., Walker, G.D., Morgan, M.V. *et al.* 2008. Fluoride and casein phosphopeptide-amorphous calcium phosphate, *J Dent Res.*, 87, 344-8
- Reynolds, E.C., Cai, F., Shen, P., Walker, G.D. 2003. Retention in plaque and remineralization of enamel lesions by various forms of calcium in a mouthrinse or sugar-free chewing gum, *J Dent Res.*, 82, 206-11
- Srinivasan, N., Kavitha, M., Loganathan, S.C. 2010. Comparison of the remineralization potential of CPP–ACP and CPP–ACP with 900 ppm fluoride on eroded human enamel: An in situ study, *Archives of Oral Biology*, 55, 541-4
- Ten Cate, J.M. 1999. Current concepts on the theories of the mechanism of action of fluoride, *Acta Odontol Scand.*, 57, 325-9

\*\*\*\*\*